SUPPLEMENTARY DATA

Highly reactive crystalline phase embedded strontium-Bioactive nanorods for multimodal bioactive applications.

D. Durgalakshmi[a,d], R. Ajay Rakkesh[b], M. Kesavan[b], S. Ganapathy[b,c*], T.G. Ajithkumar[c], S. Karthikeyan[d] and S. Balakumar[a]

[a.] *National Centre for Nanoscience and Nanotechnology, University of Madras, Chennai, India.*
[b.] *CAS in Crystallography & Biophysics, University of Madras, Chennai, India.*
[c.] *National Chemical Laboratory, Homi Bhabha Road, Pune 411008, India.*
[d.] *Department of Medical Physics, Anna University, Chennai, India.*
[#]Corresponding author, balasuga@yahoo.com

1. Internal structure of the nanorods:

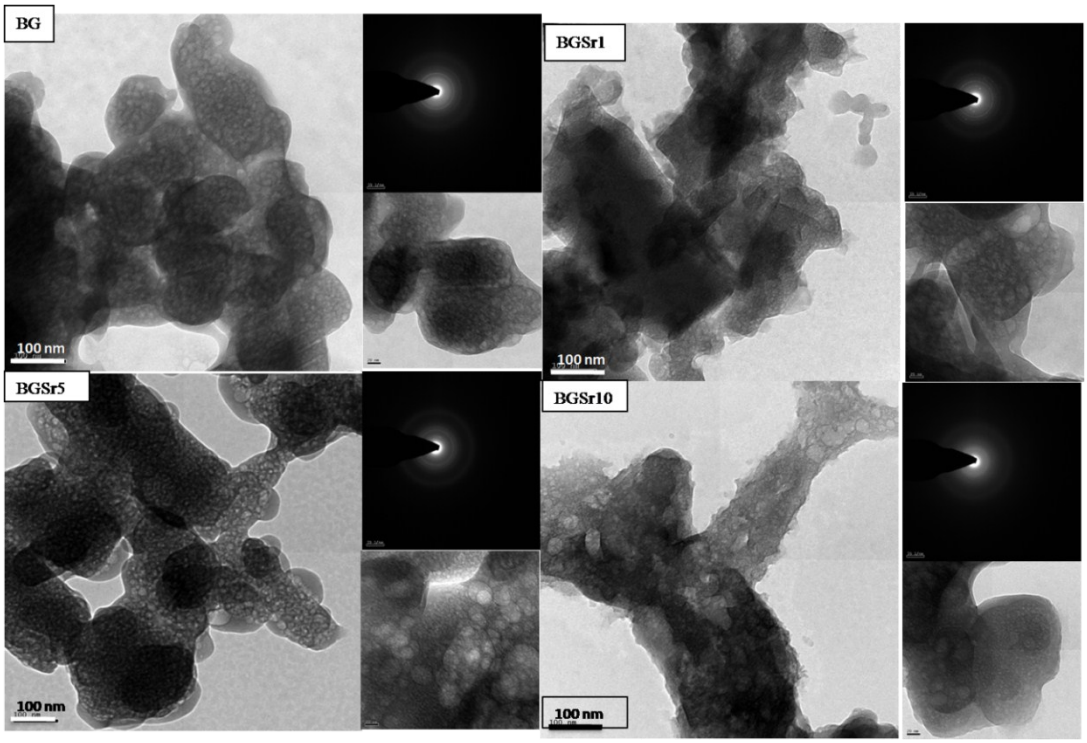

Fig S1. Internal structure morphology and the respective SAED pattern of BG and strontium substituted Bioactive material

The internal structure of the nanorods shows a lot of porous structures and the SAED pattern confirms the amorphous nature of the material. Increase in the strontium% there leads to higher porous size inside the rod structure. In general, the higher porous material leads to higher degradation rate due to its higher surface area.

2. Porosity Analysis:

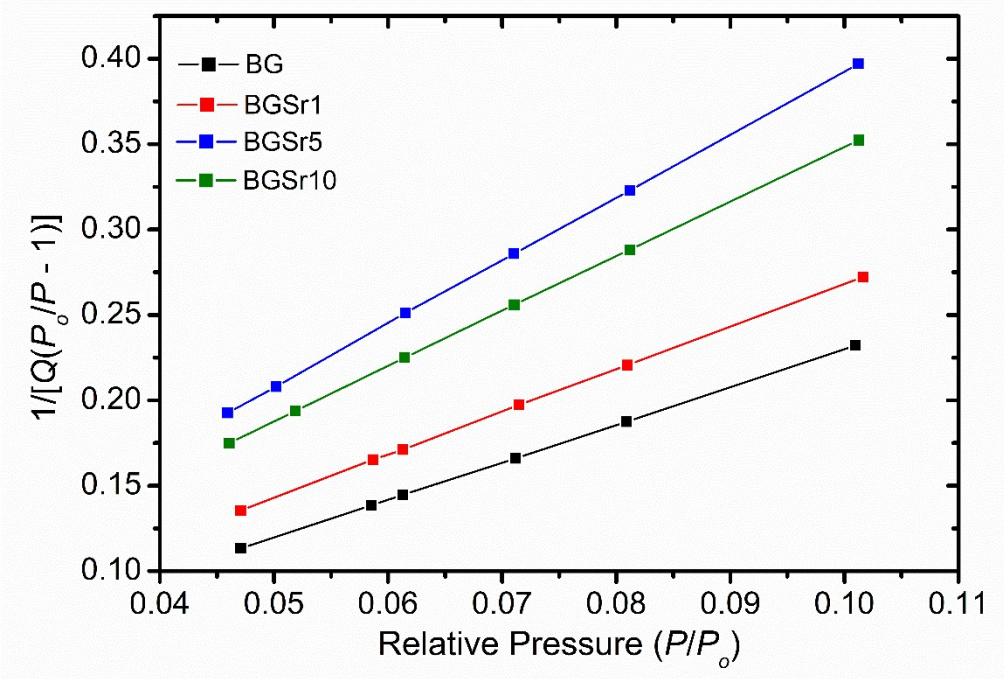

Fig. S2 BET multipoint surface area analysis

The BET surface areas of all materials were calculated from the nitrogen and argon isotherms in Fig. S2. The BET surface areas were obtained using the consistency criteria. The Brunauer-Emmet-Teller (BET) equation is given as,

$$\frac{1}{Q[(P_o/P)-1]} = \frac{1}{X_m C} + \frac{C-1}{X_m C}\left(\frac{P}{P_o}\right)$$

using this equation and information from the isotherm, the surface area of the sample was measured. In the equation where Q is the weight of the nitrogen adsorbed at the given relative pressure (P/P_o), X_m is monolayer capacity, which is the volume of gas adsorbed at standard temperature and pressure (STP), and C is constant [1]. When BET equation is plotted, the graph should be linear with a positive slop for obtaining the surface area. The linear plot given in Figure S1 satisfies the consistency criterion and good fit. The obtained parameters were given in Table S1. The results show that a Surface area and pore volume decreases with increase in strontium substitution in Bioactive material. However, the pore size is less for BGSr5 and higher pore volume depicts that it will be suitable for higher interaction in vivo when used for dentin applications.

Sample	BET Surface Area (m^2/g)	Pore Volume (cm^3/g)	Pore Size nm
BG	1.9679	0.017375	111.78
BGSr1	1.7262	0.11632	157.21
BGSr5	1.6990	0.008948	98.71
BGSr10	1.3424	0.008190	123.99

Table S1: Porosity analysis of Bioactive material and Strontium Substituted Bioactive material

Table S2 : Atomic Coordinates from Rietveld Refinement of XRD Data of Bioactive material BG

Phase 1 Name: Combeite

Atom	x	y	z
Na1	0.34857	0.98239	0.57846
Ca2	0.34857	0.98239	0.57846
Na3	0.32939	1.34824	0.68363
Ca4	0.32939	1.34824	0.68363
Na5	0.47866	0.35992	0.71972
Ca6	0.50124	0.36788	0.15972
Na7	0.50124	0.36788	0.15972
Ca8	0.85015	0.00000	0.83333
Ca9	0.26608	0.00000	0.33333
Si10	0.26556	0.27483	0.76001
Si11	0.46048	0.31822	0.88373
Si12	0.60716	0.10920	0.76190
O13	0.10812	0.00000	0.83333
O14	0.73681	0.00000	0.83333
O15	0.45166	0.40297	0.90004
O16	0.54581	0.21717	0.76122
O17	0.40800	0.27207	0.86122
O18	0.36581	0.25767	0.10183
O19	0.61482	0.05729	0.68488
O20	0.07587	0.16013	0.78940
O21	0.60401	0.52870	0.83929
O22	0.74851	0.20861	0.83036

Phase 2 Name: Clinophosinaite

Atom	x	y	z

Na1	0.00000	0.53202	0.25000
Na2	0.00000	0.17002	0.25000
Na3	0.50000	0.11952	0.75000
Na4	0.50000	0.18697	0.25000
Na5	0.50000	0.43391	0.25000
Na6	0.50000	0.50000	0.00000
Na7	0.51133	0.18226	0.00562
Na8	0.30379	0.39735	0.38854
Na9	0.23193	0.01171	0.09154
Ca10	0.00000	0.50000	0.00000
Ca11	0.00000	0.12284	0.75000
Ca12	-0.00455	0.21220	0.50697
Si13	0.32905	0.35200	0.65422
Si14	0.33142	0.34200	0.83261
P15	0.29006	0.30043	0.15306
P16	0.22719	0.04714	0.37249
O17	0.24286	0.18355	0.67569
O18	0.20416	0.34419	0.52726
O19	0.45324	0.41294	0.91024
O20	0.20170	0.39657	0.74459
O21	0.20040	0.47700	0.87498
O22	0.15521	0.27288	0.84703
O23	0.34439	0.24123	0.09538
O24	0.20167	0.30258	0.27617
O25	0.09116	0.34399	0.08358
O26	0.38814	0.39994	0.08864
O27	0.27946	0.22253	0.40652
O28	0.00837	0.10179	0.83743
O29	0.51510	0.08556	0.29946
O30	0.60424	0.12730	0.89109
O31	0.32310	0.00273	0.32891
O32	0.32436	0.00960	0.93548
O33	0.21505	0.01699	0.26193

3. Immersion studies:

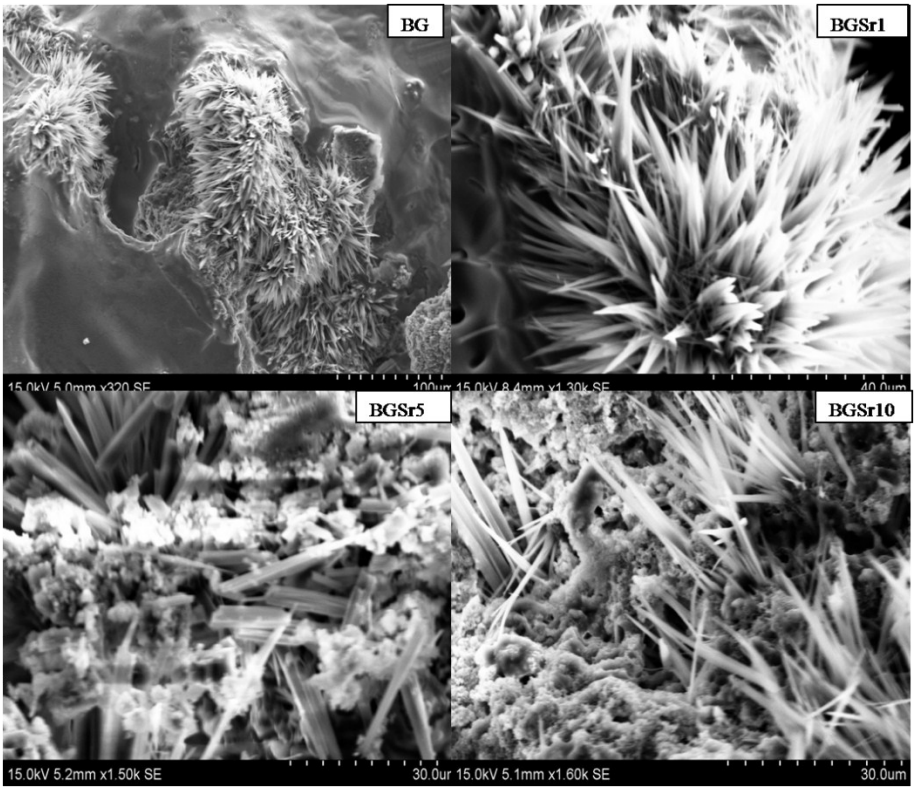

Fig. S3 SEM images of Bioactive material and strontium substituted Bioactive material after immersion

In order to understand the Biocompatibility of the samples, the samples have been made in the form of a pellet and immersed in simulated body fluid (ASTM G5-94) for 14 days. The change in the surface morphology and Hydroxyapatite formation has been confirmed from SEM and XPS. The procedure for immersion studies has been followed by Kokubo et al.[3] BG shows a sheeted layer over the sample surface and needle formation was observed in the entire sample (Fig. 3). As the increase in the strontium percentage, there occurs a disintegration of the samples and it is covered by HA crystal which was further confirmed by XPS analysis.

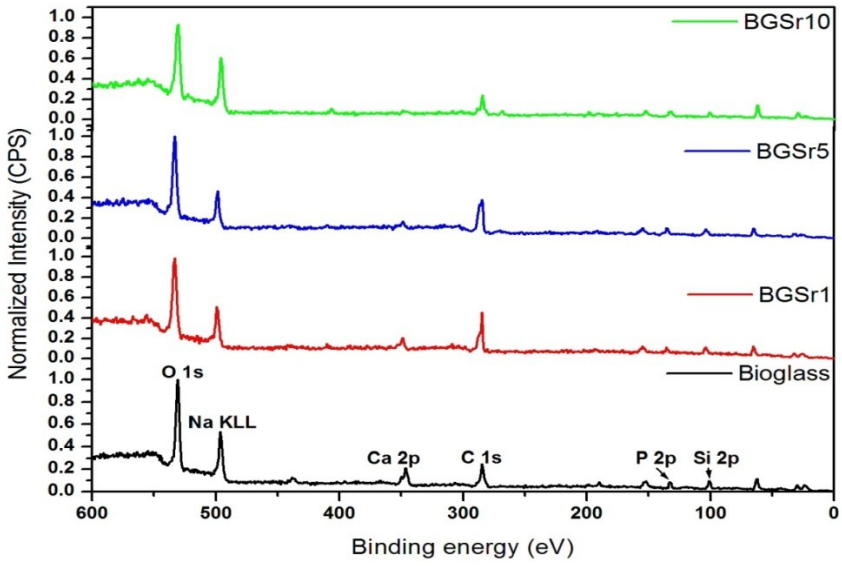

Fig. S4 XPS survey spectrum of BG and strontium substituted Bioactive material after immersion

XPS spectra for Bioactive material after immersion shows an increase in calcium and phosphate peak compare to the before immersion samples attribute to the HA formation of the samples. The higher intensity of the BG is due to the sheeted uniform structure compare to strontium substituted samples.

4 Antimicrobial studies

The samples were made into pellets of 8 mm diameter using a hydraulic press and used for this study. Before examination of the antimicrobial studies, the samples were sterilized under UV light for 20 mins. *Enterococcus faecalis* (*E.Faecalis*) bacterial strain was isolated from the human teeth of the patients in Sri Ramachandra Medical College, Chennai. *Escherichia coli* (E.Coli) strain was procured from ATCC and used for this study. Muller Hilton agar (Hi-media, India) is used as a growth medium and Millipore water is used as dilution media. The bacterial strains were diluted up to the turbidity of 0.5 Mc Farland standards and spread plated over the agar medium. The samples were placed on the agar and incubated overnight and the zones of inhibition were measured as per rules of Kirby Bauer disc diffusion method.

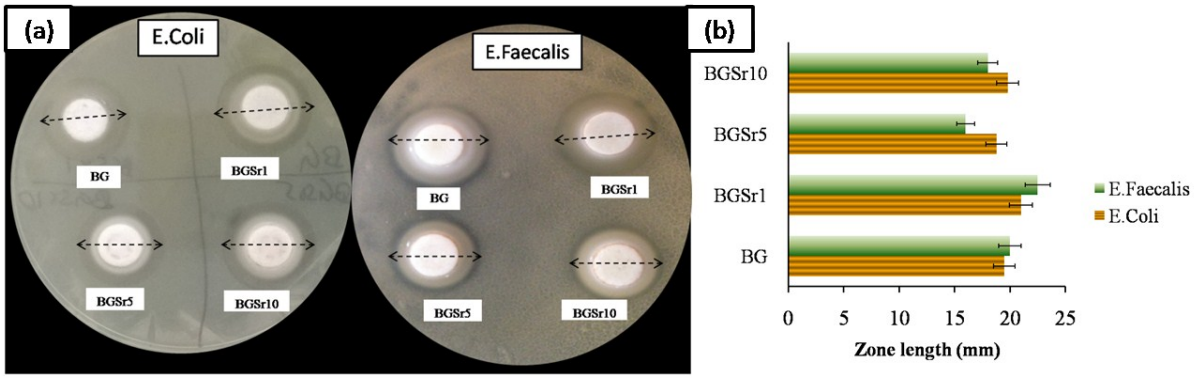

Fig. S5 Antimicrobial efficacy of Bioactive material and strontium-substituted Bioactive material against E. Coli and E. faecalis bacterial strain.

The anaerobic gram-negative E. faecalis and E. Coli microorganisms were the prime microorganisms present in the root canal of the teeth [4]. The tooth regenerative material used also has antibacterial property otherwise it leads to rejection of the material at the earlier stage itself. Hence the antimicrobial efficacy of these clinically stained microorganisms has been tested against Bioactive material and strontium-substituted Bioactive material for Bioactive material (BG), BGSr1, BGSr5 and BGSr10 as shown in Fig. 5. The white region near to the pellet surface shows degradation of the samples and the zone was measured up to the transparent region. The lower concentration of 1wt% substituted Bioactive material (BGSr1) is also taken for antibacterial studies to understand the effect of bacterial at lower concentrations. The result indicates that BGSr5 shows higher antimicrobial efficacy as compared to the other samples. This could be due to the smaller structure of BGSr5 having the higher surface area, leads to higher interaction and antibacterial activity on the bacterial strains.

4. Dentin matrix studies

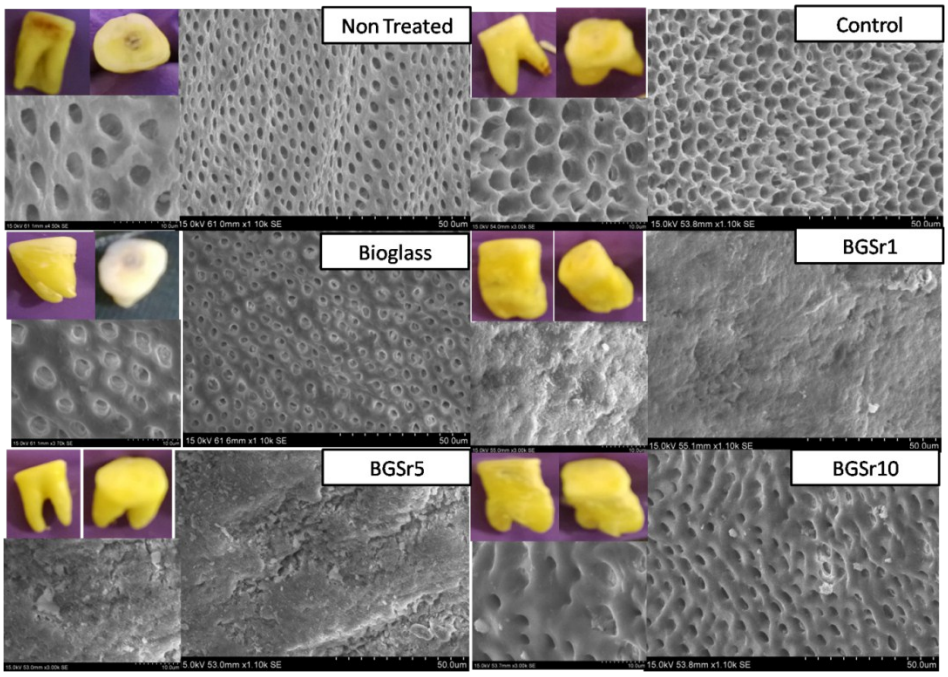

Fig. S6 Surface morphology and dentin surface after polished with Bioactive material and Strontium Bioactive material and immersed in artificial saliva for one day.

The dentin tubules were completed covered by the samples after one-day treatment itself. The BGSr1 and BGSr5 samples completely occluded the tubules due to its smaller size of the particles and which will enhance the rate of dentin regeneration.

Table S3: Molecular docking parameters of Bioactive material and Strontium Bioactive material (PDP ID: 3APV)

Compound name	Hydrogen bond (D-H...A)	Distance Å	Binding Score Kcal/mol
Bioactive material	Na5…O(Glu 64)	2.4	-16.70
	Si10-O13…N(Arg 68)	3.5	
	Si11-O18…O(Glu 92)	3.0	
	Si11-O21…N(Arg 90)	2.7	
	Si11-O21…N(Arg 90)	2.9	
	Si12-O22…O(Glu 64)	2.4	
	Si12-O14…O(Gln 66)	2.6	
	Si12-O19…N(Gln 66)	2.1	
BGSr5	(Glu 64)O-H…Na1	3.1	-24.14
	(Glu 64)O-H…Na1	3.4	
	(P15)-O25…N(Gln 66)	2.6	
	(P15)-O23…O(Gln 66)	2.6	
	(Glu 92)O-H…Na3	2.6	
	(Glu 92)O-H…Na5	3.0	
	(Glu 92)O-H…Na5	2.4	
	(Ser 40)O-H…Na6	3.1	

	(Ser 40)O-H…Na7	3.1	
	(Glu 92)O-H…Na8	2.7	
	(Gln 66)O-H…Na9	3.3	
	(Si14)-O21…O(Asn 75)	2.0	
	(Si13)-O33…N(Arg 68)	3.1	
	(P16)-O29…N(Arg 68)	3.2	
Bgsr10	(Glu 64)O-H…Ca10	3.4	-19.13
	(Asn 75)O-H…Ca12	2.3	
	(Glu 64)H-N…Na2	3.5	
	(Gln 66)H-O…Na2	2.9	
	(Ser 40)H-O…Na7	3.5	
	(Gln 66)H-O…Na9	3.1	
	P16-O29…N(Arg 68)	3.1	
	P16-O28…N(Arg 68)	3.4	
	P15-O24…O(Gln 66)	2.6	
	Si13-O18…N(Arg 90)	2.9	
	Si13-O18…N(Arg 90)	3.0	
	Si14-O19…O(Asn 75)	1.4	
	Si14-O21…O(Asn 75)	2.3	
	Si14-O22…N(Arg 90)	3.3	

5. Thermal analysis

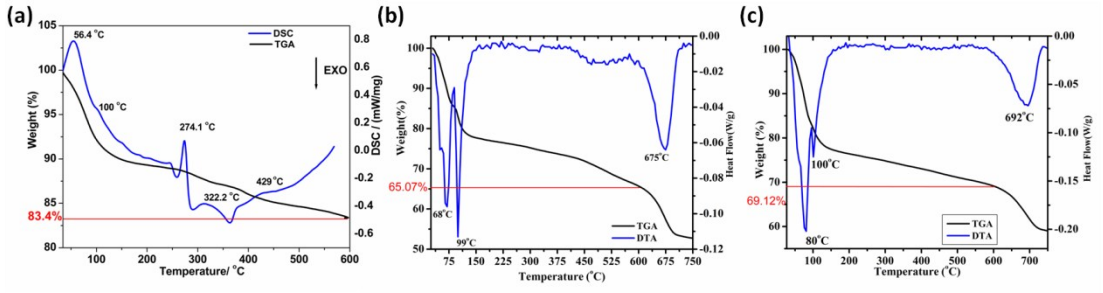

Fig. S7 (a) TGA-DSC spectrum of Bioactive material, TGA-DTA spectra of (b) BGSr5 and (c) BGSr10.

The thermal behaviour of the samples was analysed using TGA-DSC analysis for Bioactive material and TGA-DTA analysis of BGSr5 and BGSr10 using thermal gravimetric analysis (NETZCH, Germany) at the heating rate of 10K/min in a nitrogen atmosphere using platinum crucible. The five major transitions in TGA-DSC is for Bioactive material, BGSr5 and BGSr10. For Bioactive material, the first transition is up to 200°C in TGA and corresponding endothermic peak in DSC is attributes to the aqueous loss in the sample. The second and third transitions from 200°C to 400°C and 400°C to 600°C and two endothermic peaks in each transition shows the phase transition and crystallization of the material. This strongly suggests that multiple crystallization is observed when the material is heat treated in the region from 200°C to 500°C. The TGA transitions were observed to be similar for all the samples; however, the residual mass at 600 °C is varying as 83.4%, 65.07% and 69.12% for bioactive material, BGSr5 and BGSr10 respectively. This transition trend is similar to the particle size variation as discussed in surface morphology analysis. In DTA analysis of BGSr5 and BGSr10, two sharp endothermic peaks were observed below 100°C corresponds

to the evaporation of the volatile hydoxyl and organic compounds. In order to understand the significant effect of uniform transformation in the material, the optimum sintering temperature for all the samples was chosen to be at 600°C, for stable glass network formation and lesser crystallization of the material.

6. Elemental analysis

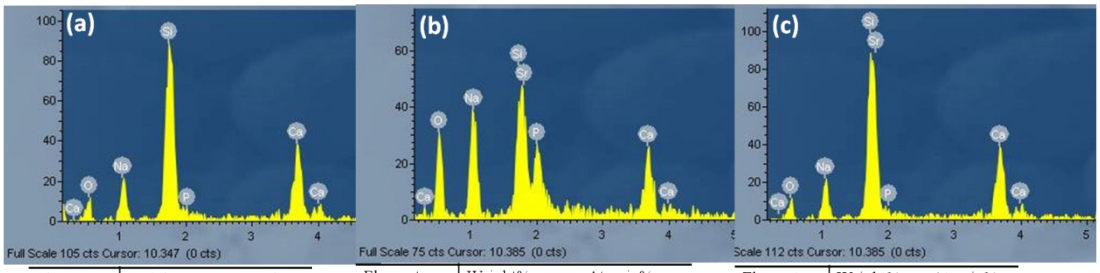

Element	Weight%	Atomic%
O K	28.89	43.08
Na K	12.68	13.16
Si K	35.25	29.94
P K	0.14	0.11
Ca K	23.04	13.71
Totals	100.00	

Element	Weight%	Atomic%
O K	51.06	64.86
Na K	12.01	6.05
Si K	24.11	21.31
P K	1.41	1.86
Ca K	6.66	4.82
Sr L	4.77	1.11
Totals	100.00	

Element	Weight%	Atomic%
O K	46.08	62.12
Na K	10.16	7.30
Si K	24.70	21.42
P K	1.63	1.49
Ca K	11.35	5.62
Sr L	7.07	3.15
Totals	100.00	

Fig. S8 EDS of (a) Bioactive material, (b) BGSr5 and (c) BGSr10 and its respective elemental composition.

As per the principle of EDS, the surface within 5µm only we can understand the chemical composition of the sample. Also, the presence of oxygen will greatly alter the remaining composition of the sample. EDS for sintered and the results are given in Fig. S8. On eliminating the oxygen%, the atomic percentages of the individual elements were approximately equal to the mol % of the samples as given in table 5. The slight variation might be due to the in situ low range order crystallization in the scanning region. However, the variation in the Sr substitution on ca is clearly varied with an increase in concentration.

Table S4: Composition of Bioactive material in mol%

Sample code		SiO_2	NaO	CaO	SrO	P_2O_5
BG	mol%	46.13	24.35	26.92	-	2.60
BGSr5	mol%	47.33	24.98	21.97	3.05	2.67
BGSr10	mol%	48.59	25.64	16.77	6.26	2.74

References

[1] Brunauer S, Emmett PH, Teller E: Adsorption of gases in multimolecular layers. *Journal of the American Chemical Society,* 60(2) *(*1938):309-319.

[2] T. Kokubo, H. Takadama, *Biomaterials*, 27 (2006) 2907-2915.